metals

MDPI

Article

Removal of Mg and MgO By-Products through Magnesiothermic Reduction of Ti Powder in Self-Propagating High-Temperature Synthesis

Sang Hoon Choi [1,2], Jae Jin Sim [1], Jae Hong Lim [1,2], Seok-Jun Seo [1], Dong-Wook Kim [3], Soong-Keun Hyun [2] and Kyoung-Tae Park [1,*]

1 Korea Institute for Rare Metals, Korea Institute of Industrial Technology, Incheon 21999, Korea; csh33@kitech.re.kr (S.H.C.); simjae@kitech.re.kr (J.J.S.); cow1boy@kitech.re.kr (J.H.L.); sjseo@kitech.re.kr (S.-J.S.)

2 Department of Advanced Materials Engineering, In-Ha University, Incheon 22212, Korea; skhyun@inha.ac.kr

3 Department of Chemical Engineering, In-Ha University, Incheon 22212, Korea; dwkim86@inha.ac.kr

* Correspondence: ktpark@kitech.re.kr; Tel.: +82-32-458-5199

Received: 2 January 2019; Accepted: 29 January 2019; Published: 1 February 2019

Abstract: Commercial production of titanium involves chlorination using chlorine gas that can be converted to hydrochloric acid by atmospheric moisture and is hazardous to human health. In the titanium production process, self-propagating high-temperature synthesis is one of the process to directly reduce titanium dioxide. In this work, titanium powder was prepared by self-propagating high-temperature synthesis using titanium dioxide as the starting material and magnesium powder as a reducing agent. After the reaction, magnesium and magnesium oxide by-products were then removed by acid leaching under different leaching conditions, leaving behind pure Ti. During each leaching condition, the temperature of the leaching solution was carefully monitored. After leaching, the recovered titanium in the form of a powder was collected, washed with water and dried in a vacuum oven. Detailed compositional, structural, and morphological analyses were performed to determine the presence of residual reaction by-products. It was found that leaching in 0.4 M hydrochloric acid followed by second leaching in 7.5 M hydrochloric acid is the optimum leaching condition. Furthermore, it was also noticed that total volume of solution in 0.4 M hydrochloric acid leaching condition is advantageous to maintain uniform temperature during the process.

Keywords: titanium powder; self-propagating high-temperature synthesis; acid leaching; magnesium; magnesium oxide

1. Introduction

Titanium (Ti) is commonly used in the aerospace, chemical, petrochemical, maritime, and biomedical fields due to its outstanding properties, including low density, high corrosion resistance, high specific strength, and biocompatibility [1,2]. Commercially, titanium is produced using the Kroll process, which is based on the magnesiothermic reduction of titanium tetrachloride ($TiCl_4$) [2,3]. While the Kroll process can produce high-quality titanium, it is a batch-type process and is therefore costly, has a low productivity, and presents an environmental hazard because of the release of chlorine gas [4]. For these reasons, researchers have been attempting to replace the Kroll process with new titanium production processes such as the Fray Farthing Chen (FFC) Cambridge process [5], Ono and Suzuki (OS) process [6], preform reduction process (PRP) [7], Armstrong process [8,9], and hydrogen-assisted magnesiothermic reduction (HAMR) process [10].

Titanium dioxide (TiO_2) is used as a raw material in the FFC, OS, PRP, and HAMR processes, while $TiCl_4$ is used in the Kroll and Armstrong processes. TiO_2 is safer to handle and easier to

transport than $TiCl_4$, which is a highly toxic chemical. Therefore, when using TiO_2, it is less important for the Ti metal production plant and raw material production plant to be in close proximity to each other [10]. In addition, in the 1990s, it was reported that $TiCl_4$ is one of the most dangerous water-reactive substances because hydrogen chloride gas forms when liquid $TiCl_4$ reacts with atmospheric moisture [11]. However, TiO_2 is much more difficult to reduce than $TiCl_4$ because the Ti-O and Ti-Ti bonding energies have a high chemical affinity for oxygen at 2.12 eV and 2.56 eV, respectively [10,12].

In the processes described above, magnesium (Mg) and calcium (Ca) are used as reducing agents. Oxides such as MgO and CaO, as well as residual Mg and Ca, are present as by-products and must be removed by leaching. For example, in the PRP process, Ca vapors are used as the reducing agent. In the leaching process, acetic acid (CH_3COOH), and hydrochloric acid (HCl) are used as the leaching solution to remove the by-products [7]. Mg is used as a reducing agent in the HAMR process, and hydrochloric acid is used as a leaching solution to remove residual Mg and MgO [10].

In our previous work, we produced Ti powder directly from Ti dioxide by self-propagating high-temperature synthesis (SHS) using Mg as a reducing agent. After leaching, a spherical Ti powder was prepared by plasma treatment. X-ray Diffraction (XRD) images of the sample produced by the SHS process are shown in Figure 1. MgO and residual Mg were detected as reaction by-products in addition to Ti [13]. No intermediate phases such as $Ti_{10}O_9$, Ti_3O_5, or Ti_2O_3 were identified. If these intermediate phases were to be produced, it would be almost impossible to achieve reduction using Mg as a reducing agent [14].

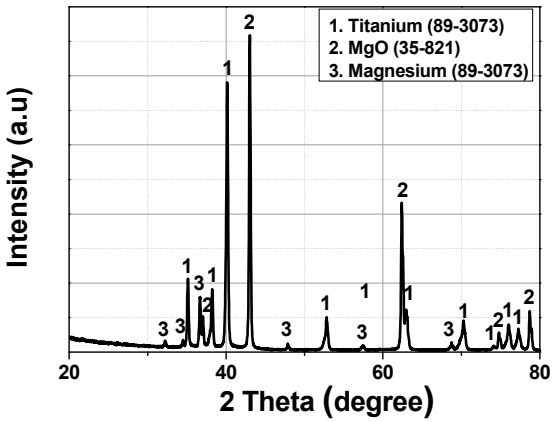

Figure 1. XRD analysis results of product of combustion synthesis of TiO_2 + 3Mg system [13].

From these points of view, SHS could be regarded as an alternative means of producing Ti metal since the process time and overall energy consumption of the SHS process are dramatically lower than those of a typical metallothermic reduction under isothermal heating conditions, given that the only energy input is that required to ignite the mixture of raw materials. In the present study, our purpose is the leaching of the products of SHS. We optimized selective leaching to remove Mg and MgO, thus leaving pure Ti powder. We have addressed the synthesis of Ti by the SHS process in a previous study [13]. Figure 1 shows the as-synthesized SHS products consisting of Ti, Mg, and MgO without any other Ti oxides, such as $Ti_{10}O_9$, Ti_3O_5, or Ti_2O_3.

2. Materials and Methods

2.1. Materials

Raw materials used in this study included: Ti powder was prepared by SHS using Titanium dioxide powder (TiO_2, 99.99 mass%, particle size 2 μm, Kojundo Chemical Laboratory Co., Ltd., Saitama, Japan) and Mg powder (Mg, >98.5 mass%, particle size <74 μm, DaeJung Chemicals and Metals Co., Ltd., Siheung, Korea) as raw materials. Acid solutions used in leaching to remove the Mg

and MgO by-products were hydrochloric acid (HCl, 35–37 mass%, Junsei Chemical Co., Ltd., Tokyo, Japan) and acetic acid (CH_3COOH, 99.5 mass% min, OCI Co., Ltd., Seoul, Korea).

2.2. Methods

Leaching was performed using a hotplate with a k-type thermocouple installed to monitor the temperature of the solution during the leaching. The by-products, Mg and MgO, were removed with an acid solution, filtered, and then washed, as illustrated in Figure 2. The leaching experiments were classified into two groups, as shown in Table 1. Group 1 was subdivided into five experiments with different conditions; however, in each case, a single leaching process was used. The five experiments differed in the concentration of hydrochloric acid (HCl) used. Group 2 was subdivided into four experiments, all of which involved a two-step leaching process. Experiment 2–1 was first conducted using CH_3COOH, followed by HCl. All the other experiments except 2–1 were first conducted using a less-concentrated hydrochloric acid, followed by a strong HCl.

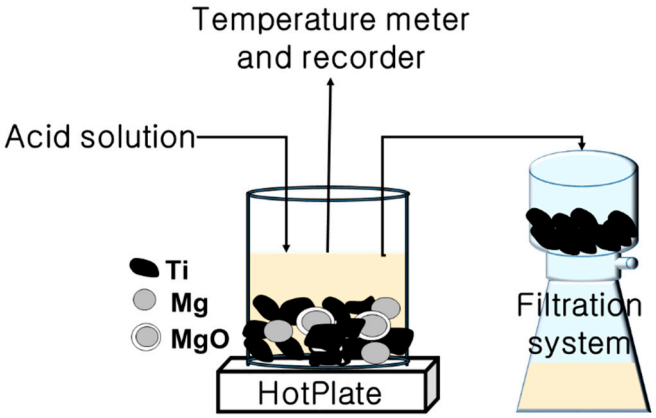

Figure 2. Leaching and filtration system for the removal of reaction by-products.

Table 1. Experimental acid leaching conditions for the removal of reaction by-products.

Group Number	Experiment Number	Step	Solvent	Concentration (M)	Amount of Product (g)	Total Volume of Solution (mL)	Stirring Time (h)	Stirring Speed (rpm)
Group 1	1–1	1	HCl	5	28	183	4	150
	1–2			5.5				
	1–3			6.5				
	1–4			7				
	1–5			7.5				
Group 2	2–1	1	CH_3COOH	8.75		183	6	
		2	HCl	6.5		183	1	
	2–2	1	HCl	0.6		183	6	
		2		6.5		183	1	
	2–3	1	HCl	0.6		183	6	
		2		7.5		183	1	
	2–4	1	HCl	0.4		3000	6	
		2		7.5		183	1	

Overall, 28 g of the SHS product was used, and the stirring speed was set as 150 rpm. After leaching, the sample was separated from the solution by filtration and then dried in a vacuum oven. After drying, the microstructure and crystallinity were determined by Field Emission-Scanning Electron Microscopy (FE-SEM, JEOL, JSM-7100F, Tokyo, Japan) and X-ray Diffraction (XRD, Bruker, D8 ADVANCE, Billerica, MA, USA with Cu-Kα radiation) analyses, while the oxygen content in the Ti

powder was determined by Oxygen Nitrogen/Hydrogen analysis (ON/H, Eltra GmbH, ONH 2000, Haan, Germany).

3. Results and Discussion

Figure 3 shows the results of XRD analysis of the product at each experimental condition of group 1. In the XRD results, Ti was determined to be the main peak at the all experimental conditions of group 1. However, MgO was detected after leaching in all experimental condition, indicating that MgO was not completely removed. In addition, $Mg(OH)_2$ phase was formed under a low concentration of HCl condition, as can be seen in Figure 3a,b.

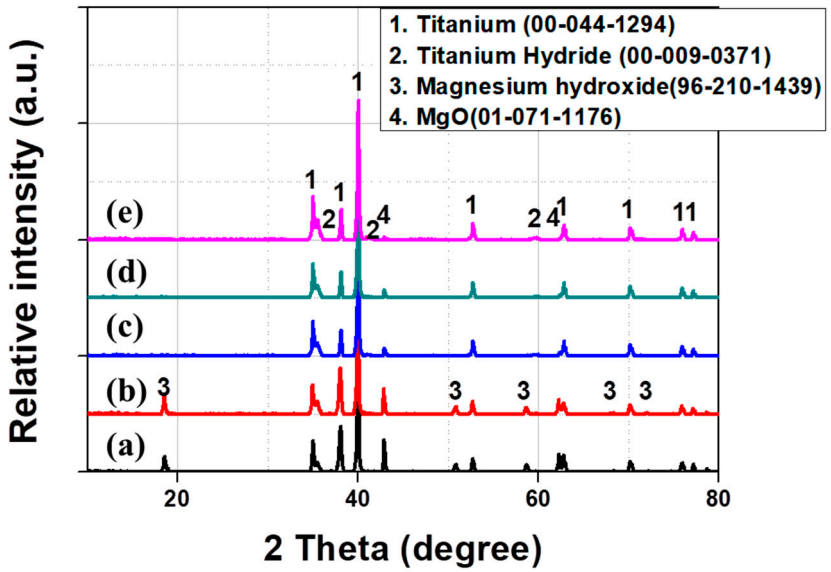

Figure 3. XRD profiles of samples obtained after leaching: (**a**) Experiment 1–1 (5 M HCl), (**b**) experiment 1–2 (5.5 M HCl), (**c**) experiment 1–3 (6.5 M HCl), (**d**) experiment 1–4 (7 M HCl), and (**e**) experiment 1–5 (7.5 M HCl).

To verify the presence of $Mg(OH)_2$, a Pourbaix diagram was drawn using the HSC Chemistry software (Chemistry Software, Houston, TX, USA) based on the pH and electrochemical potential of the Mg-H_2O system shown in Figure 4. The calculation conditions were set as 25, 50, 75, and 100 °C with a pH range of 0–14. The electrochemical potential range was set from −2 V to 2 V, relative to a standard hydrogen electrode (SHE) [15]. In the Pourbaix diagram obtained for Mg-H_2O, the inner part indicated by the dotted blue lines represents the stable region of H_2O. The area below the dotted blue lines is that in which the water is reduced and hydrogen is generated according to Equation (1). In the area above the dotted blue line, water is oxidized to generate oxygen, as defined by Equation (2).

$$2H^+ + 4e^- \rightarrow H_{2(g)} \quad (1)$$

$$2H_2O \rightarrow O_{2\,(g)} + 4H^+ + 4e \quad (2)$$

Figure 4 shows that, with an increase in the temperature from 25 °C to 100 °C, the stable region of Mg shrinks while that of the $Mg(OH)_2$ expands. Ideally, $Mg(OH)_2$ should not precipitate at pH < 8. However, as the temperature increases, $Mg(OH)_2$ can precipitate at pH < 8 at 50 °C and at pH < 7 at 100 °C.

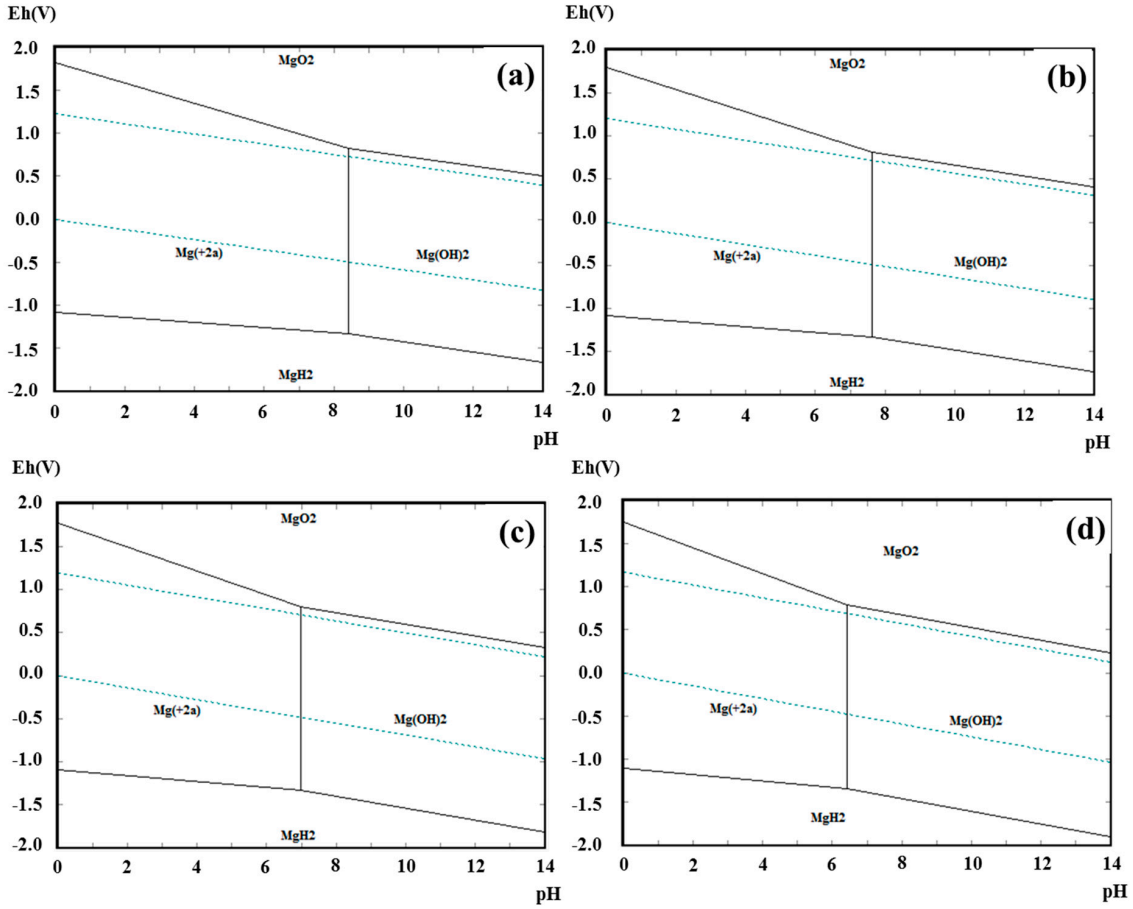

Figure 4. Pourbaix diagrams for Mg-H_2O system over a pH range of 0–14 and an electropotential range from −2.0 V to 2.0 V vs. SHE at (**a**) 25 °C, (**b**) 50 °C, (**c**) 75 °C, and (**d**) 100 °C.

The literature states that, at a lower pH, the ionizing strength of Mg^{2+} is stronger than the precipitating trace of $Mg(OH)_2$. On the other hand, at relatively higher temperatures, the amount of $Mg(OH)_2$ in the solution should gradually decrease [16]. The pH at which $Mg(OH)_2$ precipitates can be thermodynamically explained by Equations (3)–(5). The specific calculation procedure can be modified to calculate the pH using the Gibbs free energy Equation (3) and the equilibrium constant Equation (4). Using Equations (3) and (4), the pH of the solution was determined, as described in Equation (5). From Equation (5), the pH at which $Mg(OH)_2$ precipitates can be deduced from the concentration of Mg ions and the temperature of the solution system [17].

$$\Delta G^0 = -2.303RT \log_{10} K_T \tag{3}$$

where R is the ideal gas constant (8.314 $J \cdot K^{-1} \cdot mol^{-1}$), and T is the temperature as a function of the thermodynamic equilibrium quotient, K_T.

$$K_T = \frac{C_{products}}{C^0_{products}} \gamma_{products} \Big/ \frac{C_{reactants}}{C^0_{reactants}} \gamma_{reactants} \tag{4}$$

where γ is the activity coefficient, C is the concentration ($mol \cdot L^{-1}$), and C^0 is the standard concentration of 1 $mol \cdot L^{-1}$.

$$pH = \left(-\frac{\Delta G^0}{2.303RT} - log_{10}\gamma_{Mg^{2+}} \left[Mg^{2+} \right] \right) / 2 \tag{5}$$

The detection of $Mg(OH)_2$ in experiments 1–1 and 1–2 can be explained by the occurrence of an exothermic reaction during acid leaching, caused by the contact between Mg, MgO, and HCl. It is also

believed that $Mg(OH)_2$ precipitates as the pH increases due to ionization upon dissolution. $Mg(OH)_2$ precipitated only in experiments 1–1 and 1–2, and did not precipitate when a highly concentrated leaching solution was used.

The above phenomenon occurred because the pH of the leaching solution used to remove MgO and Mg was lower than that used for experiments 1–1 and 1–2. The pH can be expected to be lower than that at which $Mg(OH)_2$ precipitates, even when the pH increases during the leaching process. XRD analysis also confirmed the presence of TiH_2, which was expected to be produced by the contact between hydrogen ions in the solution and Ti. The reaction formula is given by Equation (6). The TiH_2 dehydrogenation behavior of the product was studied by several researchers who found that it is relatively easily removed by vacuum heat treatment at 700 °C [18].

$$Ti + 2H^+ + 2e^- \rightarrow TiH_2, \Delta G^0{}_{50^\circ C} = -101.769 \text{ kJ/mole} \quad (6)$$

The formation of the TiH_2 phase during leaching is disadvantageous to the processing, as additional steps will be required for its removal, thus incurring extra time and cost. On the other hand, the presence of TiH_2 is advantageous because it is insoluble in water and resistant to acidic solutions. Pure Ti metal can be easily produced through the heat treatment of TiH_2 [19].

The results of XRD analysis confirm that the MgO phase remains, regardless of the concentration of the acid. The remaining MgO is presumed to be produced by the decomposition of $Mg(OH)_2$.

For this, we confirmed the reaction occurrence from the HSC chemistry software and found that the reaction occurs at 600 °C or higher [20]. The reaction formula is given by Equation (7). This result agrees with a former report by Haoliang Dong et al., which MgO was obtained by $Mg(OH)_2$ calcined at different temperatures (500–700 °C) and durations (2–48 h) [21].

$$Mg(OH)_2 \rightarrow MgO + H_2O(l), \Delta G^0{}_{600^\circ C} = -5.269 \text{ kJ/mole} \quad (7)$$

To quantitatively measure the amount of MgO in Group 1, Rietveld refinement was applied to the TOPAS software (structure analysis software, Bruker, Billerica, MA, USA), which revealed that the concentration of MgO decreases from 1–1 to 1–4, being 19%, 15.8%, 14.22%, and 12.2%, respectively [22]. The fraction of MgO decreases as the concentration of HCl increases. It is thought that the amount of HCl used as the leaching solution was insufficient to remove Mg and MgO produced in the combustion synthesis process. A previous study removed the by-products by leaching with acetic acid, followed by rinsing with HCl [7]. We used a sufficient amount of weak acid to remove any by-products, including Mg and MgO. A second leaching step was performed using a strong acid to remove any residual impurities.

The enthalpy and Gibbs free energy of HCl and acetic acid were calculated, and the results are listed in Table 2 [20]. The calculated results show that the temperature is the same as when acetic acid is used, while the enthalpy and Gibbs free energy are higher than those obtained when HCl is used, respectively. We deduced that using acetic acid increases the driving force of the reaction. Hence, we used acetic acid for Group 2. The XRD profiles of the Group 2 reaction products are shown in Figure 5.

As mentioned above, in experiment 2–1, the by-products were first removed by using 8.75 M acetic acid, while the remaining by-products were removed using 6.5 M HCl. In experiment 2–2, the by-products were first removed using 0.6 M HCl, followed by another removal using 6.5 M HCL. The XRD analysis of the reaction products were measured and the results were compared. Under both the conditions, the MgO and Mg by-products were successfully removed; however, the Ti oxide and Ti hydride phases remained. To remove these, we replaced acetic acid with HCl.

Table 2. Calculated reaction enthalpy and Gibbs free energy with hydrochloric acid and acetic acid.

$Ti + MgO + Mg + 4HCl \rightarrow Ti + H_2O(g) + H_2(g)$			$Ti + MgO + Mg + 4CH_3COOH \rightarrow Ti + 2Mg(CH_3COO)_2 + H_2O(g) + H_2(g)$	
Temp. (°C)	ΔH (kJ)	ΔG (kJ)	ΔH (kJ)	ΔG (kJ)
10	−213.557	−328.134	−645.888	−488.862
20	−217.321	−332.114	−627.825	−483.641
30	−220.731	−335.971	−612.213	−478.991
40	−223.968	−339.720	−598.095	−474.830
50	−227.133	−343.366	−584.942	−471.104
60	−230.256	−346.915	−572.584	−467.772
70	−233.373	−350.370	−560.828	−464.802
80	−236.525	−353.734	−549.498	−462.168
90	−239.732	−357.008	−538.522	−459.850
100	−243.019	−360.193	−527.840	−457.830

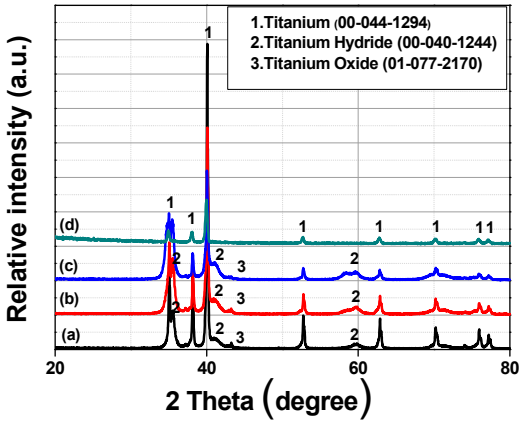

Figure 5. XRD profiles of reaction products: (**a**) experiment 2–1 (8.5 M CH_3COOH, 6.5 M HCl), (**b**) experiment 2–2 (0.6 M HCl, 6.5 M HCl), (**c**) experiment 2–3 (0.6 M HCl, 7.5 M HCl), and (**d**) experiment 2–4 (0.4 M HCl, 7.5 M HCl).

Experiment 2–3 was essentially the same as experiment 2–2, with the first leaching process performed using 0.6 M HCl. In the second step, the concentration of HCl was slightly higher than that used in experiment 2–2 (i.e., 7.5 M). The resulting product was subjected to XRD analysis (Figure 5). Similar to experiments 2–1 and 2–2, in experiment 2–3, the Mg and MgO peaks were not detected, while the Ti oxide and Ti hydride phases were still present.

In all the three experiments, we detected Ti oxide, which was not detected after the combustion synthesis. As shown in Figure 6a–c, when acetic acid and HCl were used, the temperature increased sharply during the acid-leaching process. This was caused by an exothermic reaction that occurred when MgO and Mg surrounding the Ti exothermically reacted with each other. MgO melted and the heat was transferred to the Ti surface, which reacted with the oxygen ions present in the solution to form an oxide film on the Ti powder surface. This is presumed to be the reason for the detection of Ti oxide. Figure 7 is a schematic illustration of Ti oxide formation.

To confirm the formation of Ti oxide under all the three conditions and to control the exothermic reaction, the concentration of acid used in the first leaching step was decreased from 0.6 M to 0.4 M. Similarly, to control the temperature, distilled water was used. In the second leaching step, 7.5 M HCl was used in the same way as in experiment 2–3. The XRD profile of the product (Figure 5d) show that Ti oxide was not formed because an exothermic reaction did not occur during the reaction, while MgO and Mg were completely removed. Here, a single Ti phase was detected.

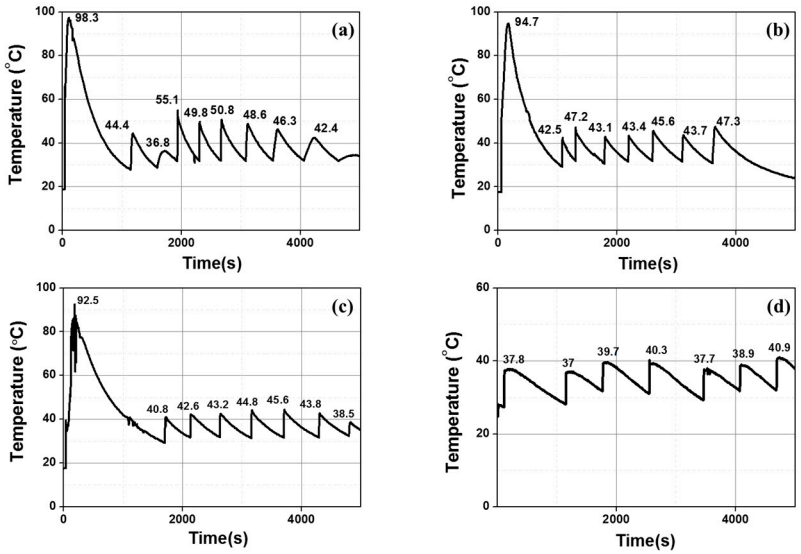

Figure 6. Temperature of leaching solution during two-step acid leaching process: (**a**) experiment 2–1 (8.5 M CH_3COOH, 6.5 M HCl), (**b**) experiment 2–2 (0.6 M HCl, 6.5 M HCl), (**c**) experiment 2–3 (0.6 M HCl, 7.5 M HCl), and (**d**) experiment 2–4 (0.4 M HCl, 7.5 M HCl).

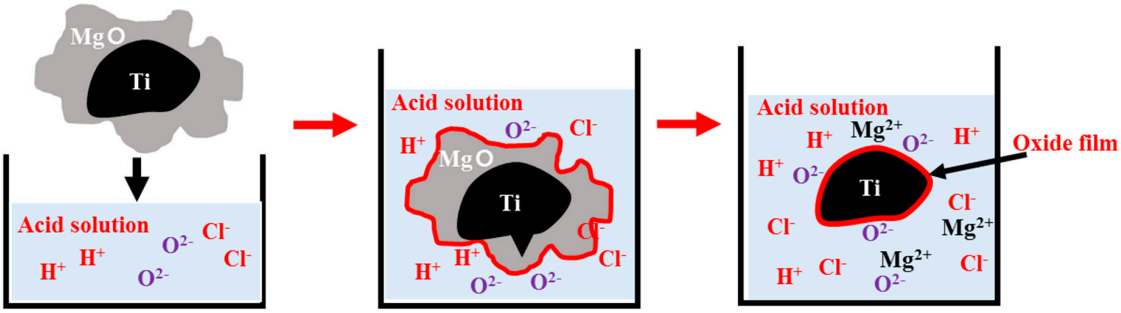

Figure 7. Ti oxide formation during leaching in experiments 2–1 to 2–3.

To identify the morphology of the reaction product and its purity, a sample produced in experiment 2–4 was subjected to FE-SEM and EDS analyses. The results of the analysis are shown in Figure 8. The prepared Ti powder exhibited an irregular shape, and the EDS results revealed that the Ti powder contained no impurities at all.

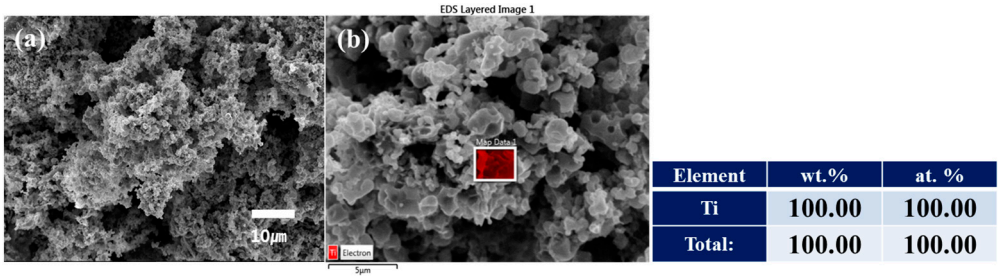

Figure 8. Morphology and purity of reaction product of experiment 2–4 (0.4 M HCl, 7.5 M HCl): (**a**) FE-SEM image and (**b**) EDS analysis result.

The oxygen contents of the Ti powders prepared according to Groups 1 and 2 leaching experimental conditions were measured using an NO/H analyzer. The results are shown in Figure 9. The concentration of MgO under each condition was about 10–19%, as mentioned above, for the first experiment. The second group of experiments also led to the formation of Ti oxides through an exothermic reaction between the reaction by-products and the acid solution in experiments 2–1 to 2–3,

resulting in a remarkably high oxygen value. However, Ti oxide was not formed once the exothermic reaction was controlled by increasing the amount of distilled water used in experiment 2–4, and all the by-products were removed, leaving only the Ti single phase with an oxygen content of about 1.0 wt%.

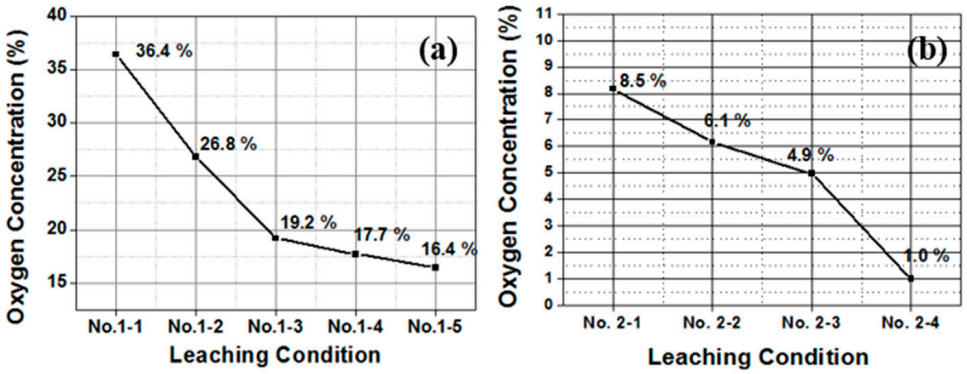

Figure 9. Oxygen contents of Ti powders as final product produced under experimental conditions of (**a**) Group 1 and (**b**) Group 2.

However, during acid leaching, where it is necessary to prepare the Ti powder when Ti oxide is formed, the reduction to Ti metal was very difficult in experiments 2–1 to 2–3. For example, Ti oxides such as TiO_2 have been reported to be more difficult to reduce because the Gibbs free energy required for reduction to Ti metal is 0.83 times less than that required for TiO_2 [14]. Nersisyan et al. reported that the oxygen content of Ti powder after SHS and leaching with nitric acid was 1.5 wt%. To further decrease the oxygen content, they performed deoxygenation with Ca. After deoxygenation, they found that the oxygen content had decreased to about 0.2–0.3 wt% [2]. Similarly, Okabe et al. reported that the oxygen content was 0.28 wt% for the Ti powder prepared using the PRP process [7]. For comparison, the Ti powder prepared in the present study had an oxygen content of about 1 wt% immediately after acid leaching and without any further steps.

4. Conclusions

Removal of by-products including Mg and MgO was studied using the magnesiothermic reduction of Ti powders in an SHS process. Ti oxide was used as the raw material and Mg was used as the reducing agent. To remove any unnecessary by-products such as Mg and MgO, acid leaching was used. HCl was chosen as the leaching solution and the efficiency of leaching was estimated by varying the concentration of the HCl. It was determined that two-step leaching with HCl effectively removed the by-products. In the first step, a low concentration of HCl was used, while a high concentration was used in the next step. Acid leaching with HCl is simpler than the conventional process in which complex experimental variants are used. The total oxygen content of the Ti powder immediately after leaching was found to be about 1 wt%, which is thought to be an advantage in terms of process simplicity and economy. The use of heat treatment would further lower the oxygen content.

The authors intend to undertake further in-depth studies to confirm the location of the remaining oxygen. That is, we will confirm whether the oxygen exists on the surface of the Ti powder or as an interstitial impurity. This will be the subject of a future report.

Author Contributions: S.H.C.: Investigation, methodology, writing—original draft; J.J.S.: Investigation; J.H.L.: Software; S.J.S.: Resources; D.W.K.: Validation; S.K.H.: Supervision; K.-T.P.: Funding acquisition, project administration, writing—-review & editing.

Funding: This research was funded by the Technology Innovation Program (Grant No. 10063427) funded by the Ministry of Trade, Industry & Energy and partially funded by an internal R&D program of the Korea Institute of Industrial Technology (KITECH) funded by the Ministry of Strategy and Finance, Republic of Korea.

Conflicts of Interest: The authors declare no conflict of interest.

References

1. Won, C.W.; Nersisyan, H.H.; Won, H.I. Titanium powder prepared by a rapid exothermic reaction. *Chem. Eng. J.* **2010**, *157*, 270–275. [CrossRef]
2. Nersisyan, H.H.; Won, H.I.; Won, C.W.; Jo, A.; Kim, J.H. Direct magnesiothermic reduction of titanium dioxide to titanium powder through combustion synthesis. *Chem. Eng. J.* **2014**, *235*, 67–74. [CrossRef]
3. Zheng, H.; Okabe, T.H. Selective chlorination of titanium ore and production of titanium powder by preform reduction process (PRP). In Proceedings of the 16th Iketani Conference, Tokyo, Japan, 12–16 November 2006.
4. Zheng, H.; Okabe, T.H. Production of titanium powder directly from titanium ore by preform reduction process (PRP). In Proceedings of the 5th UT^2 Graduate Student Workshop (University of Tokyo-University of Toronto), Tokyo, Japan, 7 June 2006.
5. Chen, G.Z.; Fray, D.J.; Farthing, T.W. Direct electrochemical reduction of titanium dioxide to titanium in molten calcium chloride. *Nature* **2000**, *47*, 361–363. [CrossRef]
6. Suzuki, R.O.; Ono, K.; Teranuma, K. Calciothermic reduction of titanium oxide and in-situ electrolysis in molten $CaCl_2$. *Metall. Mater. Trans. B* **2003**, *34*, 287–295. [CrossRef]
7. Okabe, T.H.; Oda, T.; Mitsuda, Y. Titanium powder production by preform reduction process (PRP). *J. Alloys Compd.* **2004**, *364*, 156–163. [CrossRef]
8. Chen, W.; Yamamoto, Y.; Peter, W.H.; Gorti, S.B.; Sabau, A.S.; Clark, M.B.; Nunn, S.D.; Kiggans, J.O.; Blue, C.A.; Williams, J.C.; et al. Cold compaction study of Armstrong process Ti-6Al-4V powders. *Powder Technol.* **2011**, *214*, 194–199. [CrossRef]
9. Chen, W.; Yamamoto, Y.; Peter, W.H.; Clark, M.B.; Nunn, S.D.; Kiggans, J.O.; Muth, T.R.; Blue, C.A.; Williams, J.C.; Akhtar, K. The investigation of die-pressing and sintering behavior of ITP CP-Ti and Ti-6Al-4V powders. *J. Alloys Compd.* **2012**, *541*, 440–447. [CrossRef]
10. Xia, Y.; Fang, Z.Z.; Zhang, Y.; Lefler, H.; Zhang, T.; Sun, P.; Huang, Z. Hydrogen assisted magnesiothermic reduction (HAMR) of commercial TiO_2 to produce titanium powder with controlled morphology and particle size. *Mater. Trans.* **2017**, *58*, 355–360. [CrossRef]
11. Kapias, T.; Griffiths, R.F. Accidental releases of titanium tetrachloride ($TiCl_4$) in the context of major hazards-spill behavior using REACTPOOL. *J. Hazard. Mater.* **2005**, *A119*, 41–52. [CrossRef] [PubMed]
12. Okabe, T.H.; Hamanaka, Y.; Taninouchi, Y. Direct oxygen removal technique for recycling titanium using molten $MgCl_2$ salt. *Faraday Discuss.* **2016**, *190*, 109–126. [CrossRef] [PubMed]
13. Choi, S.H.; Ali, B.; Hyun, S.K.; Sim, J.J.; Choi, W.J.; Joo, W.; Lim, J.H.; Lee, Y.J.; Kim, T.S.; Park, K.T. Fabrication of a spherical titanium powder by combined combustion synthesis and DC plasma treatment. *Arch. Metall. Mater.* **2017**, *62*, 1057–1062. [CrossRef]
14. Bolivar, R.; Friedrich, B. Synthesis of titanium via magnesiothermic reduction of TiO_2 (pigment). In Proceedings of the EMC, Kyoto, Japan, 20–24 July 2009.
15. HSC Chemistry Software ver. 8.0, Eh-pH Diagrams Module, Outotec. 2014. Available online: https://www.outotec.com (accessed on 20 November 2018).
16. Brown, P.L.; Ekberg, C. *Hydrolysis of Metal Ions*; Wiley-VCH: Weinheim, Germany, 2016; pp. 180, 194.
17. Won, Y.R.; Kim, D.S. Studies on the effect of temperature on lead ion in aqueous environment based on pourbaix diagram. *J. Korea Soc. Waste Manag.* **2013**, *30*, 60–67. [CrossRef]
18. Qian, M.; Froes, F.H. *Titanium Powder Metallurgy: Science, Technology and Applications*; Elsevier Inc.: Amsterdam, The Netherlands, 2015.
19. Fang, Z.Z.; Middlemas, S.; Guo, J.; Fan, P. A new, energy-efficient chemical pathway for extracting Ti metal from Ti minerals. *J. Am. Chem. Soc.* **2013**, *135*, 18248–18251. [CrossRef] [PubMed]
20. HSC Chemistry Software ver. 8.0, Reaction Equations Module, Outotec. 2014. Available online: https://www.outotec.com (accessed on 20 November 2018).

21. Dong, H.; Unluer, C.; Al-Tabbaa, A.; Yang, E.H. Characterization of MgO Calcined from $Mg(OH)_2$ Produced from Reject Brine. In Proceedings of the Fourth International Conference on Sustainable Construction Materials and Technologies, Las Vegas, NV, USA, 7–11 August 2016.
22. TOPAS Software ver. 5.0, Rietveld Refinement Module, Bruker. 2014. Available online: https://www.bruker.com/products/x-ray-diffraction-and-elemental-analysis/x-ray-diffraction/xrd-software/topas.html (accessed on 17 August 2018).